DESIGN OF THE ESS ACCELERATOR

H. Danared, European Spallation Source ESS AB, Box 176, SE-221 00 Lund, Sweden
for ESS/AD and the ESS/ADU Collaboration

Abstract

A conceptual design of the 2.5 GeV proton linac of the European Spallation Source, ESS, was presented in a Conceptual Design Report in early 2012. Work is now progressing towards a Technical Design Report at the end of 2012. Changes to the linac configuration during the last year include a somewhat longer DTL and a change to fully segmented cryomodules. This paper reviews the current design status of the accelerator and its subsystems.

INTRODUCTION

Top-level requirements on the linac of the European Spallation Source include that it should accelerate 50 mA of protons to 2.5 GeV in pulses that are 2.86 ms long and come with a repetition rate of 14 Hz. This implies that the average beam power on the target will be 5 MW and the peak power 125 MW. The linac will have a normal-conducting front-end up to 79 MeV followed by three families of superconducting cavities and a high-energy beam transport to the spallation target. The design as of autumn 2011 is described in a Conceptual Design Report [1], and a more detailed Technical Design Report will be produced by the end of 2012.

The past year has seen the linac evolve in many respects. The medium-energy beam transport, MEBT, is becoming better defined, allowing space for chopping, collimation and beam instrumentation. The drift-tube linac, DTL, has a FODO structure and is extended from 50 to 79 MeV to improve beam dynamics. Cryomodules of the superconducting linac have become fully segmented, and the current baseline (May 2012) has spoke cryomodules with two double-spoke cavities per module, medium-beta modules with four five-cell elliptical cavities and high-beta modules also with four five-cell cavities. Warm quadrupole doublets are located between each cryomodule in the spokes and medium-beta sections and between every second module in the high-beta section. The linac tunnel has come closer to the surface which somewhat changes the layout of the high-energy beam transport, HEBT. One modulator for two klystrons and one klystron per cavity is now foreseen. In order to fit the klystrons into the RF gallery, they are positioned in groups across the gallery.

ESS is still in the Design Update phase, however, and further changes can be expected before the project enters the Construction phase. This is expected to happen in early 2013.

With high-beta cryomodules consisting of only four cavities, which match present prototyping capacities at IPN-Orsay and CEA-Saclay better than the previously foreseen 8-cavity modules, and thus are expected to save time for the project, the current baseline linac,

Table 1: Selected Linac Parameters as of May 2012

Parameter	Device	Value
Length (m)	LEBT	2.1
	RFQ	5.0
	MEBT	3.5
	DTL	32.5
	Spokes	58.6
	Medium beta	113.9
	High beta	227.9
No. of cryomodules	Spokes	14
	Medium beta	15
	High beta	30
Cavities per module	Spokes	2
	Medium beta	4
	High beta	4
Optimal beta Geometrical beta	Spokes	0.50
	Medium beta	0.67
	High beta	0.92
Transition energy (MeV)	Source–RFQ	0.075
	RFQ–DTL	3
	DTL–spokes	79
	Spokes–medium beta	201
	Medium–high beta	623

FDSL_2012_05_15, has main parameters according to Table 1.

BEAM DYNAMICS

Changes to the beam dynamics during the last year [2] are mainly due to a higher energy out of the DTL, a change in the synchronous phase at the frequency jump between spokes and elliptical cavities and modified dimensions of the cryomodules due to the segmentation and a more mature cryomodule design.

A DTL is a compact accelerating device, and at the previous output energy of 50 MeV it had a significantly shorter transverse focusing period than the spoke cryo-modules. With a longitudinal phase advance limited by the transverse period length, the result was a discontinuity in longitudinal phase advance per metre and a consequent emittance growth – and, more seriously, halo growth – at the transition to the spokes section. Extending the DTL to about 80 MeV almost eliminates the discontinuity in phase advance, and the emittances in all three planes are now nearly constant throughout the linac, see Fig. 1.

A small gain in overall acceleration efficiency has been achieved by gradually making the synchronous phase more negative before the frequency jump from 352 to 704 MHz at the exit of the spokes section. This results in stronger longitudinal focusing and shortened bunches that are better matched to the 704 MHz buckets, and thereby the accelerating gradients in the beginning of the medium-beta section can be increased.

The parameters in Table 1 are the result of an optimization for minimum linac length, and thereby minimum number of RF sources and maximum power to beam per cavity on average, given dimensions of relevant components, rules of thumb for phase advances, etc., as described in [3]. In addition, a bias has been given to a slightly reduced geometrical beta of the medium-beta cavities and a reduction of the range of particle betas in these cavities in order to reduce their sensitivity to unwanted cavity modes like $4\pi/5$.
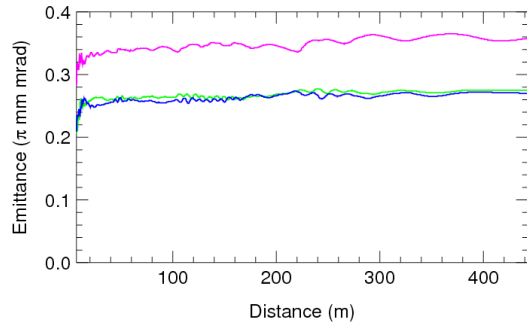

Figure 1: Normalized RMS emittances from the entrance of the MEBT to the end of the high-beta elliptical section in horizontal (green), vertical (blue) and longitudinal (violet) planes. The input distribution, at the entrance of the MEBT, is a 6D Gaussian truncated at 3 sigma with 0.21/0.21/0.28 π mm mrad.

The fundamental passband modes could prove to be dangerous due to their high R/Q compared to the accelerating modes at certain velocities. In some cases, the R/Q of the $4\pi/5$ mode is 3 times that of the fundamental at the beginning of the medium-beta section.

To explore the effect of these modes, a drift-kick-drift model was employed [4]. A pulse train of one million point-like bunches is tracked through the superconducting section of a linac, calculating the energy and time error generated by beam-induced modes. The size of the error depends on the size of the frequency spread of the modes. The spread is modelled as a Gaussian with a width given by an empirical formula [5]. One thousand linacs with different seeds for the Gaussian spread are used.
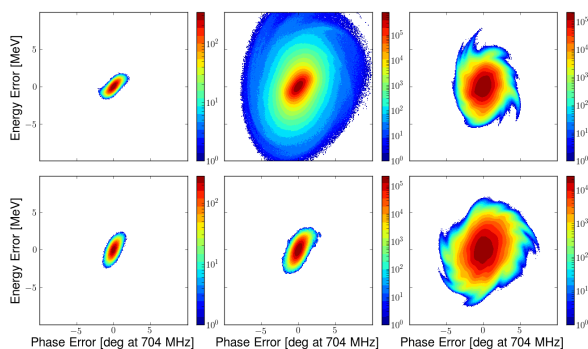

Figure 2: Pulse phase space at exit of two linacs (upper and lower rows) when no modes are acting (left), passband modes are acting (middle), there are uniformly distributed RF errors (right).

Figure 2 shows the effect of these modes on the pulse phase space of two linacs with different velocity partitioning over the three cavity families [6]. Each column shows the phase space at the exit of the linac. Of concern is when the growth due to passband modes (middle column) with respect to the case when no modes are acting (left column) is larger than that produced by acceptable RF errors (right column).

It can be seen that the linac of the top row, which represents an earlier ESS layout, is susceptible to these modes. The bottom row, corresponding to the present linac layout, shows significantly better performance.

HIGH-ENERGY BEAM TRANSPORT

The high-energy beam transport [7], HEBT, consists of a 100 m long section in the linac tunnel serving as upgrade space, a section bringing the beam up to the surface level, and a section at the surface level which expands the beam onto the rotating tungsten target. In addition, there is a line to a beam dump behind the upgrade space on the tunnel level. This beam dump is used for commissioning, start-up and beam tuning.

In the upgrade section, the doublet lattice continues with the same period as in the high-beta section of the accelerator. The dogleg transporting the beam 4 m up from the tunnel to the surface is achromatic and inclined at a 22 degree angle. The optics of the horizontal section to the target is designed to fulfil the requirements for the beam footprint and peak current density at the target.
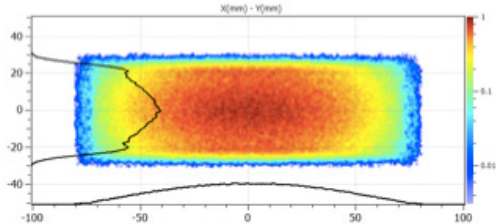

Figure 3: Example of beam profile on the target, with a peak current density of 49 $\mu A/cm^2$. The projected beam profiles are shown on a linear scale.

Octupole magnets are used to obtain a peak current density of less than 70 $\mu A/cm^2$ inside the requested footprint (160 mm × 60 mm) while keeping the power deposited outside the footprint low. In order to obtain a maximum effect of the octupoles and to keep the motion in the two planes decoupled, the expansion section has been designed so that a high ratio between the vertical and horizontal beam sizes is obtained at the position of the octupoles. Three quadrupoles are placed downstream of the last octupole in order to spread the now folded beam over the desired footprint area.

Figure 3 shows a beam profile on the surface of the target for a case where the peak current density is 49 $\mu A/cm^2$ at the target for octupole gradients of 2500 and 5000 T/m^3. In spite of the non-linear elements, not all particles will end up within the 160 mm × 60 mm footprint. For this reason, a fixed collimator will be

placed upstream of the target region, intercepting large-amplitude particles.

BEAM INSTRUMENTATION

A comprehensive suite of beam instrumentation is important to efficiently commission and operate the ESS accelerator. Beam intensity, position, longitudinal and transverse dimensions, as well as halo and beam losses need to be measured at several locations along the machine, and the proper beam distribution on target need to be verified. Minimization of beam loss and associated machine activation will be of prime importance for the operation. Transverse beam size measurement and longitudinal bunch length measurement are some of the particular diagnostics challenges. Due to the high intensity, a shortened pulse with lower repetition rate will be needed for some invasive diagnostics devices. A more detailed discussion on ESS beam diagnostics can be found in a separate paper in these proceedings [8].

RF SYSTEMS

The design of the system used to provide the accelerating RF has reached quite an advanced level but remains in a conceptual stage. Table 2 shows the requirements for each of the subsystems that the RF systems will provide power to.

Table 2: RF Parameters

Module	Frequency (MHz)	No. of couplers	Max power (kW)
RFQ	352.21	1	900
DTL	352.21	4	2150
Spokes	352.21	28	280
Medium beta	704.42	60	560
High beta	704.42	120	850

An illustration of the section of the RF klystron gallery used to provide power to the superconducting sections of the linac (i.e. the spoke, medium beta, and high beta sections) is shown in Fig. 4, and it can be seen that it has been decided to use klystrons as the power amplifier for the majority of the linac. The high voltage power is converted from the mains input through the use of modulators, and the klystron power output is then transmitted to the cavities via waveguides through penetrations in the floor of the gallery.

A trade-off between the size and cost of the modulator as a function of the stored energy has resulted in a decision to power two klystrons from each modulator.

Due to space constraints, as well as schedule considerations, the initial preference was to connect multiple cavities to a single klystron, especially in the sections of the linac that require a lower power to be transmitted to the beam. Considerations of the required phase and amplitude control of the cavity field, and the difficulties of providing such vector control for the high power RF, led to the conclusion that a solution using one cavity per klystron is preferable.
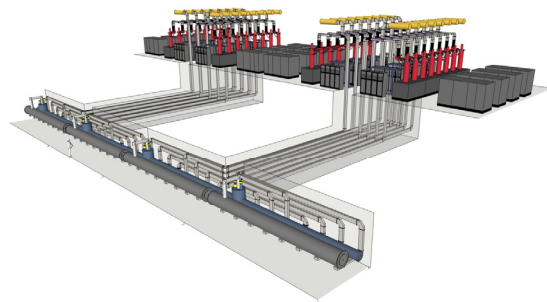

Figure 4: Layout of RF gallery (top right) and linac tunnel (bottom left) with waveguides between klystrons and cryomodules.

Until recently, the baseline plan for transmitting the RF power from the klystrons to the couplers used a separate penetration for each waveguide. Space limitations result in the dimensions of the penetrations being a very close match to those of the waveguides themselves, which means that there is no room for adding bends. Thus, such a scheme would require the waveguides to cover the necessary horizontal and vertical distance at an angle, and results in a direct line of sight from the accelerator tunnel to the gallery where staff may be working.

The proposed scheme shown in Fig. 4 allows significantly larger penetrations, thus giving the opportunity to introduce a 90 degree bend, eliminating the direct line of sight for neutron transmission.

Combined with the reduced number of penetrations, this scheme gives over an order of magnitude reduction in the expected radioactive flux observed in the gallery, and is now the preferred solution.

CONTROL SYSTEM

The Integrated Control System (ICS) has recently made significant steps forward to lay out the plans for the Construction (2013-2019) phase. ICS was identified as one of the crucial components on the critical project path. In order to follow the execution of the plans, regular cross-functional task force meetings are held continually and iterating requirements and design with the stakeholders on the hardware (timing, machine protection, Control Box [9]) and on the software (configuration management - BLED [10]).

REFERENCES

[1] ESS Conceptual Design Report, Ed. S. Peggs, ESS Report ESS-2012-1 (2012).
[2] M. Eshraqi *et al.*, These proceedings, THPPP085.
[3] M. Eshraqi *et al.*, Proc. IPAC 2011, p 2640.
[4] M. Schuh *et al.*, Phys. Rev. ST Accel. Beams **14** (2011) 051001.
[5] S. Molloy, Note, ESS Doc 92-V2.
[6] R. Ainsworth, Thesis in preparation, Royal Holloway, University of London.
[7] I.S. Holm *et al.*, These proceedings, MOPPD049.
[8] A. Jansson *et al.*, These proceedings, MOPPR045.
[9] E. Laface and M. Rescic, These Proceedings, THPPP047.
[10] J. Bobnar and K. Zagar, http://www.esrf.eu/icalepcs2011/talks/tuaault03_talk.pdf.